I. System Architecture

The system was developed using the position-domain loosely coupled closed-loop integration approach. A separate GNSS-only solution was computed using a multi-epoch GNSS Kalman filter. Another solution was computed using the dead reckoning system. The difference between both solutions is the input to the DR/GNSS Integration Kalman filter. Figure (1) describes the overview of the system architecture.

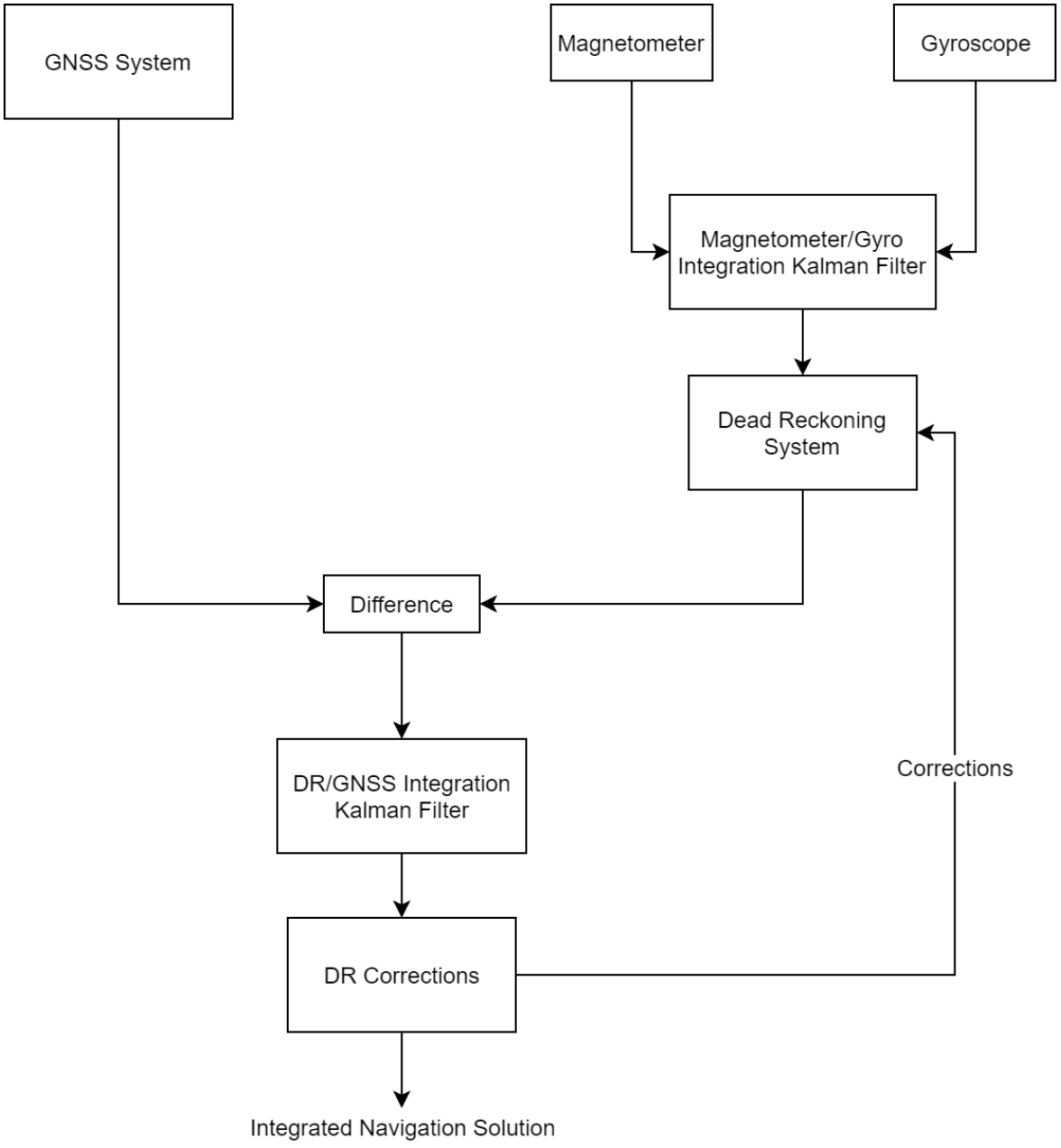

Figure (1). System Architecture

This approach was selected as it provides a separate GNSS solution which can be used for solution integrity checking, since access to the ground truth data was not provided. However, this approach is less accurate than a measurement domain tightly coupled system. This is because the Kalman filter used in the DR/GNSS integration system assumes the noise on the inputs is uncorrelated in time, which is not the case for this system as the input from the GNSS navigation system has time correlated noise, since it's Kalman filter-based. [5]

II. System Components Implementation

GNSS System

The GNSS system uses muti-epoch Kalman filter. The filter's state is initialized using a single epoch least-squares estimation, which in turn is initialized using a location in London (51.5074 °, 0.1278°), zero height, zero velocity, zero clock offset, and zero clock drift. Equations (1), (2), (3), (4), (5), (9), (10), (11), and (12) from [1] are used for the single epoch least-squares estimation. The state estimate of the multi-epoch GNSS system is

$X = \begin{bmatrix} \boldsymbol{r}_{ea}^{e} \\ \boldsymbol{v}_{ea}^{a} \\ \delta\rho_{c}^{a} \\ \delta\dot{\rho}_{c}^{a} \end{bmatrix}$, where $\boldsymbol{r}_{ea}^{e}$ is the user antenna position in ECEF frame (m), $\boldsymbol{v}_{ea}^{a}$ is the user antenna velocity in ECEF frame (m/s), $\delta\rho_{c}^{a}$ is the clock offset (m), $\delta\dot{\rho}_{c}^{a}$ is the clock drift (m/s).

The error covariance matrix is initialized as follows

$$P = \begin{pmatrix} 100 & 0 & 0 & 0 & 0 & 0 & 0 & 0 \\ 0 & 100 & 0 & 0 & 0 & 0 & 0 & 0 \\ 0 & 0 & 100 & 0 & 0 & 0 & 0 & 0 \\ 0 & 0 & 0 & 0.01 & 0 & 0 & 0 & 0 \\ 0 & 0 & 0 & 0 & 0.01 & 0 & 0 & 0 \\ 0 & 0 & 0 & 0 & 0 & 0.01 & 0 & 0 \\ 0 & 0 & 0 & 0 & 0 & 0 & 100000^2 & 0 \\ 0 & 0 & 0 & 0 & 0 & 0 & 0 & 200^2 \end{pmatrix}$$

The state transition matrix is computed as follows [2]

$$\boldsymbol{\Phi}_{k-1} = \begin{pmatrix} \mathbf{I}_3 & \tau_s\mathbf{I}_3 & \mathbf{0}_{3,1} & \mathbf{0}_{3,1} \\ \mathbf{0}_3 & \mathbf{I}_3 & \mathbf{0}_{3,1} & \mathbf{0}_{3,1} \\ \mathbf{0}_{1,3} & \mathbf{0}_{1,3} & 1 & \tau_s \\ \mathbf{0}_{1,3} & \mathbf{0}_{1,3} & 0 & 1 \end{pmatrix}$$, where the time interval is $\tau_s = 0.5s$

The system noise covariance matrix is computed as follows [2]

$$\mathbf{Q}_{k-1} = \begin{pmatrix} \frac{1}{3}S_a\tau_s^3\mathbf{I}_3 & \frac{1}{2}S_a\tau_s^2\mathbf{I}_3 & \mathbf{0}_{3,1} & \mathbf{0}_{3,1} \\ \frac{1}{2}S_a\tau_s^2\mathbf{I}_3 & S_a\tau_s\mathbf{I}_3 & \mathbf{0}_{3,1} & \mathbf{0}_{3,1} \\ \mathbf{0}_{1,3} & \mathbf{0}_{1,3} & S_{c\phi}^a\tau_s + \frac{1}{3}S_{cf}^a\tau_s^3 & \frac{1}{2}S_{cf}^a\tau_s^2 \\ \mathbf{0}_{1,3} & \mathbf{0}_{1,3} & \frac{1}{2}S_{cf}^a\tau_s^2 & S_{cf}^a\tau_s \end{pmatrix}$$

, where the acceleration power spectral density (PSD), $S_a, is\ 5\ m^2s^{-3}$, the clock phase PSD, $S_{c\phi}^a$, is $0.01\ m^2s^{-3}$ and the clock frequency PSD, S_{cf}^a, is $0.04m^2s^{-1}$.

The measurement matrix, H, and the measurement noise covariance matrix, R are computed as shown in [2] in task 2. The noise standard deviation on all pseudo-range measurements was assumed to be $\sigma_p = 10\ m$. The noise standard deviation on all pseudo-range rate measurements was assumed to be $\sigma_r = 0.05\ m/s$.

Residual based outlier detection and correction was implemented as described in [1] equations (6), (7), and (8). The threshold value used for range measurements is 5 m and the threshold value used for the range rate measurements is 1 m/s.

Magnetometer/Gyroscope Integration System

An integrated heading solution was derived using the basic open-loop integration architecture described in [3], page 39.

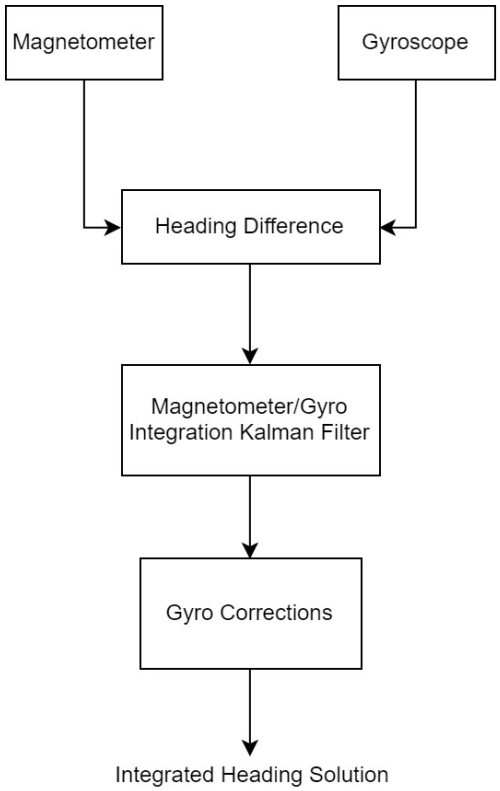

Figure (2). Magnetometer/Gyro Heading Integration

The state vector is $\boldsymbol{x} = \begin{pmatrix} \delta\psi^G \\ b_g \end{pmatrix}$, where $\delta\psi^G$ is the gyro-derived heading error and b_g is the Gyro bias.

The error covariance matrix is initialized as follows

$$P = \begin{pmatrix} deg2rad(4°)^2 & 0 \\ 0 & deg2rad(1°)^2 \end{pmatrix}$$

The measurement noise $R = \sigma_M^2 = deg2rad(4°)^2$

The gyro random noise PSD is assumed to be $S_{rg} = \left(\frac{10^{-4}}{\sqrt{3600}}\right)^2 \ rad^2 s^{-1}$ and the gyro bias variation PSD, $S_{bgd} = \ 2x10^{-12}\ rad^2 s^{-3}$.

The system noise covariance matrix, measurement matrix and the measurement innovation matrix are implemented as described in [3], pages 40 and 41.

Dead Reckoning System

The dead reckoning system is implemented as described in [4]. The mean of the 4 speed measurements from the 4 wheel speed sensors was used as the average speed of the vehicle. The instantaneous velocity of the vehicle is calculated differently from [4] using the following formula $V_k = (2-d)\bar{V} - (1-d)V_{k-1}$, with the damping factor, d, set to 0.5. The heading used in the calculations, ψ_k, is the integrated heading produced by the gyro-magnetometer integration filter.

DR/GNSS Integration Filter

The DR/GNSS integration filter described in [3] and [4] was implemented to produce an integrated navigation solution. The filter estimates the DR solution velocity and position error. These errors are fed back to the DR processor every 50 epochs and the states of the filter are reset. This is done to minimize the linearization errors.

The state vector is $X = \begin{pmatrix} \delta V_N \\ \delta V_E \\ \delta L \\ \delta\lambda \end{pmatrix}$, where $\delta V_N \ and \ \delta V_E$ are the estimated north and east velocity component errors respectively, and δL and $\delta\lambda$ are the estimated latitude and longitude errors, respectively.

The error covariance matrix is computed as shown in [4] equation (5), where the initial velocity uncertainty is assumed to be $\sigma_v = 0.1\ m/s$, and the initial position uncertainty is assumed to be $\sigma_r = 10\ m$. The state transition matrix is computed using equation (6) from [4].

The system noise covariance matrix is computed using equation (7) from [4], where the DR power spectral density is assumed to be $S_{DR} = 0.2\ m^2 s^{-3}$.

The measurement matrix is computed using equation (10) from [4]. The measurement noise covariance matrix is computed using equation (11) from [4], where the GNSS position measurements standard deviation is assumed to be $\sigma_{Gr} = 10\ m$, and the GNSS velocity measurements standard deviation is assumed to be $\sigma_{Gv} = 0.05\ m/s$/axis.

The Kalman gain matrix and measurement innovation vector are computed using equations (12) and (13) from [4] respectively. The DR solution is corrected using equation (16) from [4].

III. Results

Figure (3) shows the integrated solution result including the positions, velocity and heading of the lawnmower. Figure (4) shows the position and velocity solution without heading. Figure (5) shows the position and heading solution without velocity. Figure (6) shows the integrated position solution versus the GNSS only position solution. Figure (7) shows the GNSS position solution without outlier filtering.

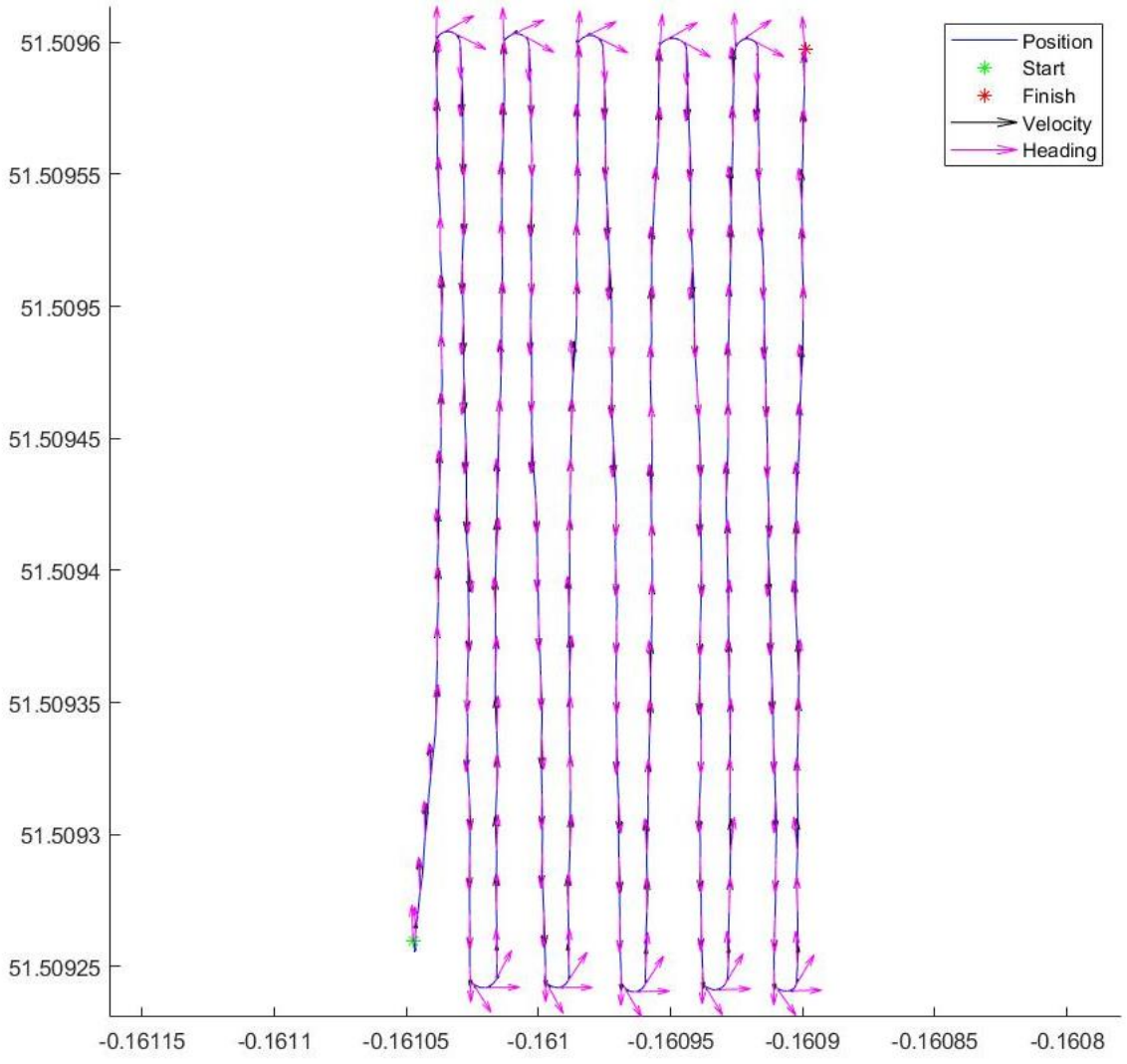

Figure (3). Integrated Solution

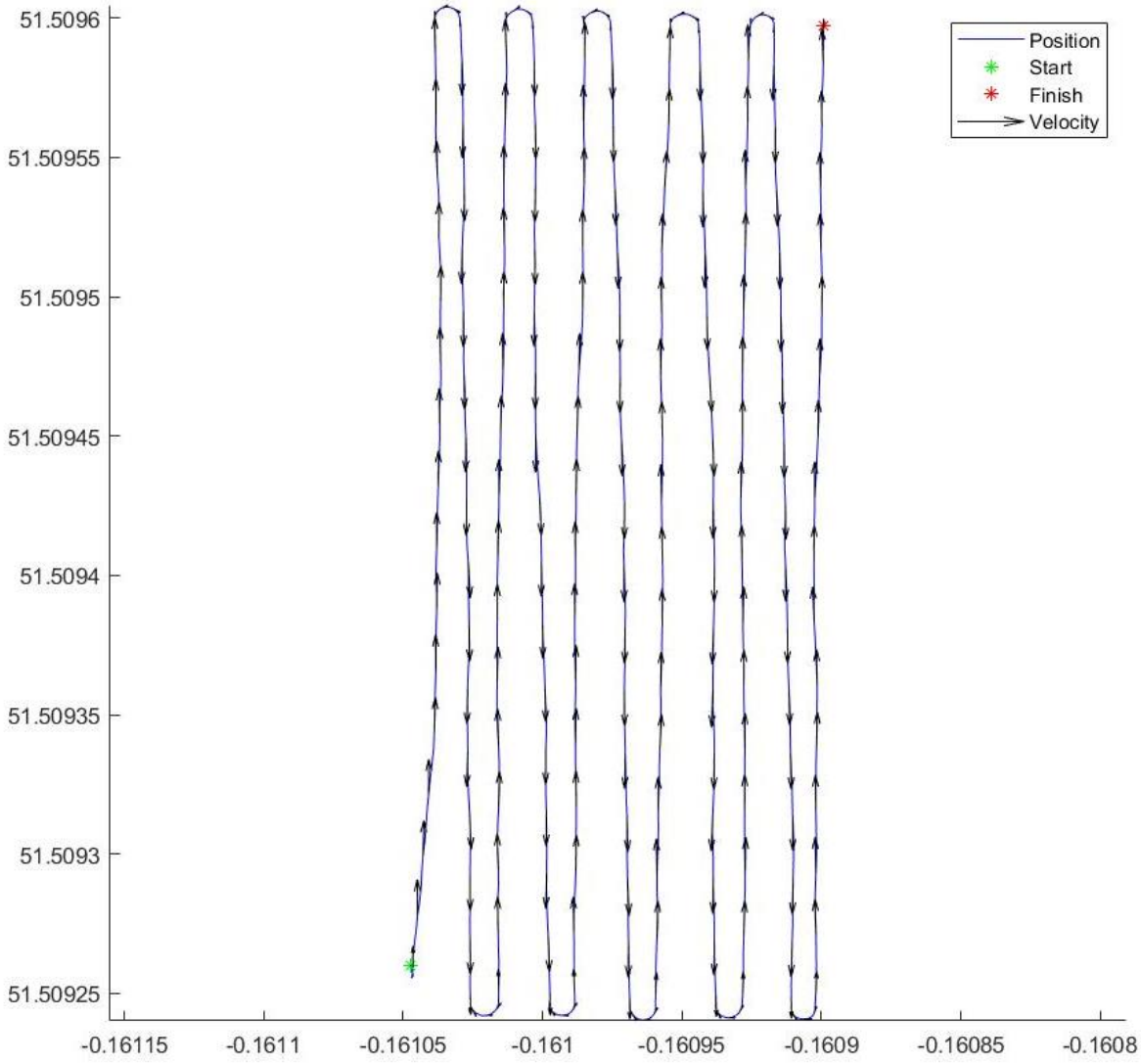

Figure (4). Velocity Solution

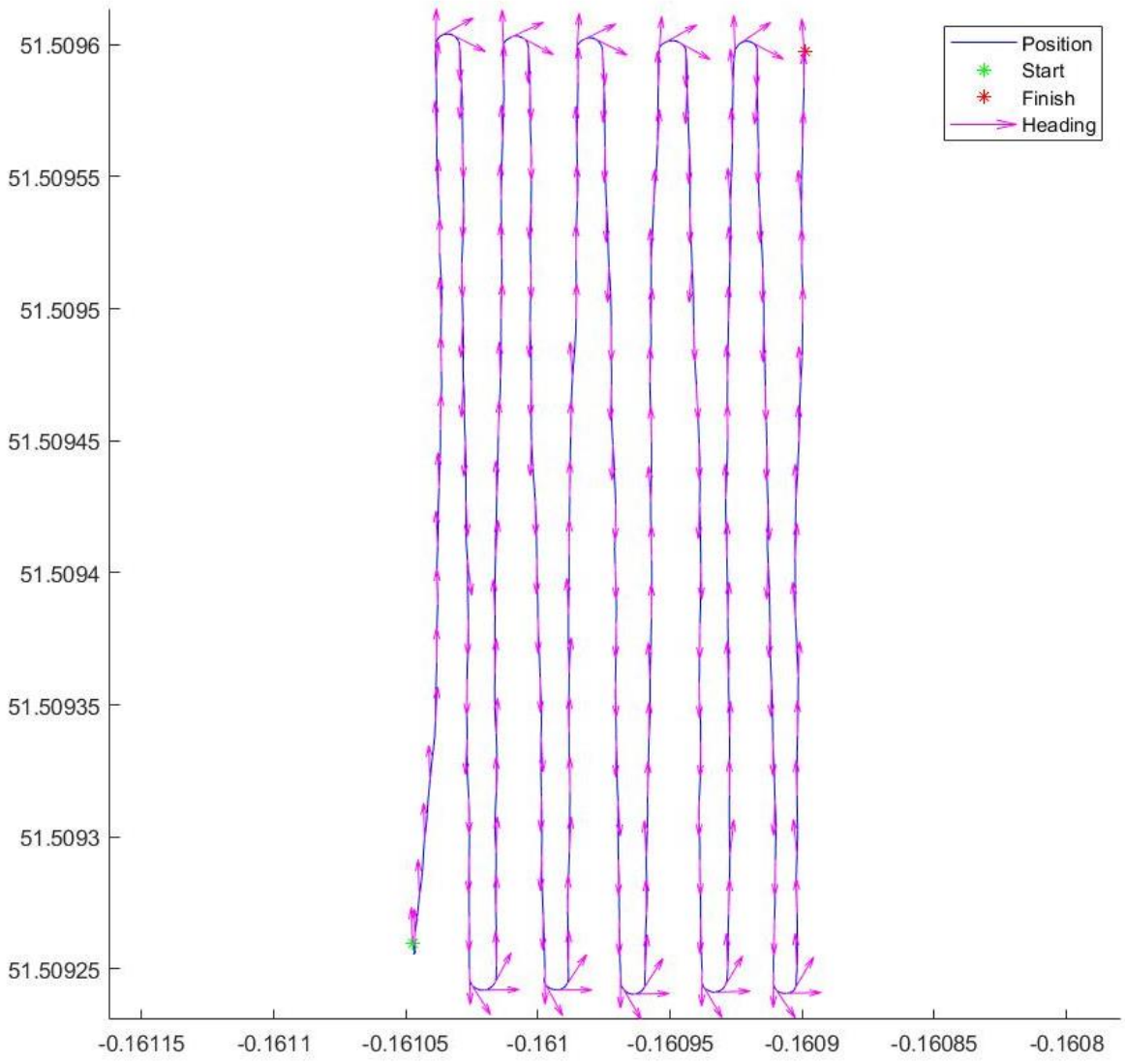

Figure (5). Heading Solution

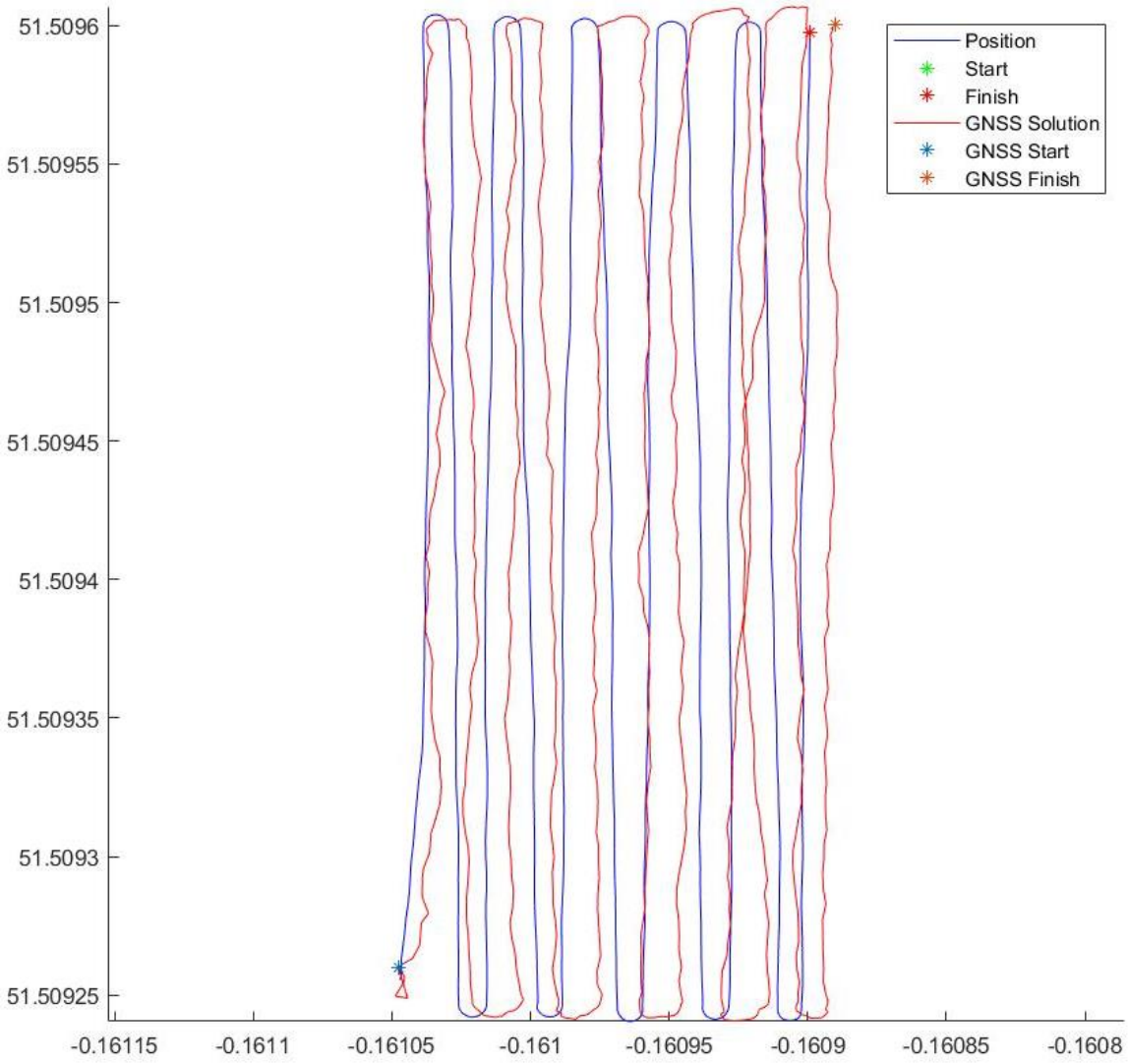

Figure (6). Integrated Position Solution vs GNSS Position Solution

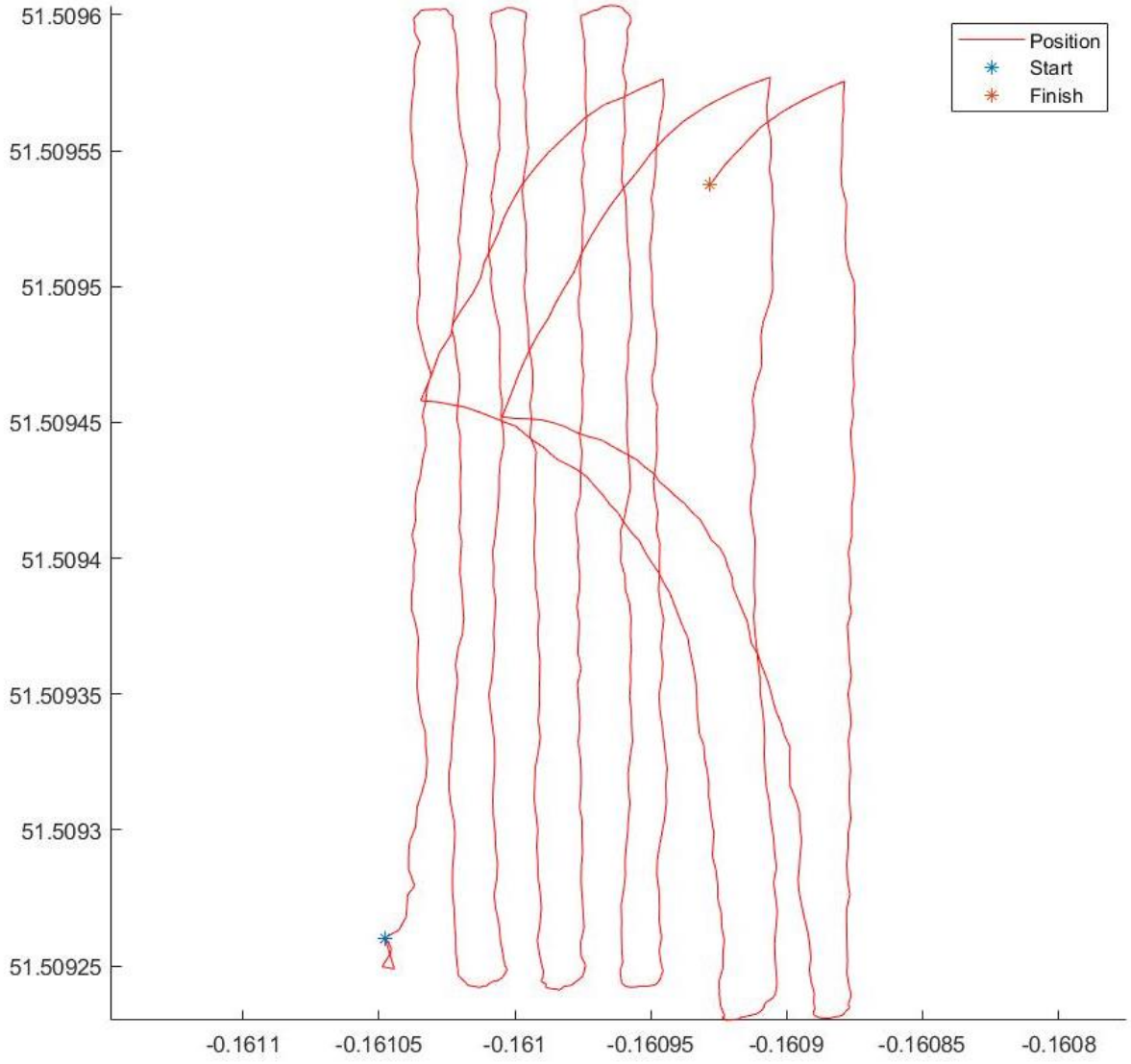

Figure (7). GNSS Position Solution Without Outlier Filtering

Results Discussion

Figure (6) shows that the integrated navigation solution produced by integrating the GNSS and DR solutions achieve the long-term accuracy of GPS whilst maintaining the smooth short-term accuracy of the DR system. Figure (7) shows the effect of outliers present on the data on the GNSS solution. Without filtering the data for outliers, large spikes in position appear in the position solution which are otherwise filtered when employing a residual based outlier filtering approach.

References

[1] COMP0130: ROBOT VISION AND NAVIGATION, Workshop1: Mobile GNSS Positioning using Least-Squares Estimation.

[2] COMP0130: ROBOT VISION AND NAVIGATION, Workshop 2: Aircraft Navigation using GNSS and Kalman Filtering.

[3] P. D. Groves, COMP0130: ROBOT VISION AND NAVIGATION, Lecture 6.

[4] COMP0130: ROBOT VISION AND NAVIGATION, Workshop 3: Multisensor Navigation.

[5] P. D. Groves, Principles of GNSS, Inertial, and Multisensor Integrated Navigation Systems, 2nd Edition, Artech House, 2013.